International Journal of Engineering Applied Sciences and Technology, 2016
Vol. 1, Issue 10, ISSN No. 2455-2143, Pages 9-18
Published Online August - September 2016 in IJEAST (http://www.ijeast.com)

MICROWAVE SYNTHESIS OF CdO AND SnO_2 NANOSTRUCTURES AND COMPARISON OF STRUCTURAL, OPTICAL AND DIELECTRIC PROPERTIES

N. Rajesh
Department of Physics, PG Assistant,
Government Higher Secondary School,
Alathur, Karur, Tamilnadu – 623131,
India

Abstract - **Potentially important metal oxides CdO and SnO_2 nanostructures were synthesized in same conditions by microwave assisted technique. The synthesized samples were characterized by XRD, TEM, EDX, UV-DRS, dielectric constant and Photoluminescence studies. The XRD pattern reveals that, CdO sample has face centered cubic structure with a preferential orientation along the (111) plane, SnO_2 sample has cassiterite-type tetragonal structure with a preferential orientation along the (110) plane. Rod like and spherical shaped nanostructures were obtained from TEM analysis for CdO and SnO_2 samples, respectively. The band gap values of CdO and SnO_2 samples were found to be 4.20 and 4 eV, respectively. Microstructural properties such as strain, dislocation density, number of crystallites; optical properties such as reflectance, refractive index, absorption coefficient, extinction coefficient, optical conductivity and dielectric properties of CdO and SnO_2 nanostructures were investigated and compared. Room temperature photoluminescence spectra of CdO and SnO_2 nanostructures also studied.**

Keywords - Microwave processing; Metal oxides; X-ray methods; Electron microscopy; Optical properties.

I. INTRODUCTION

In recent years, a wide range of metal oxides nanoparticles were synthesized to get desired chemical, electrical, mechanical and optical properties. Metal oxides have long been a subject of various investigations due to their unique physical properties and applications in commercial devices [1,2]. Metal oxides such as cadmium oxide and tin oxide have been widely studied because of their potential uses in optoelectronic devices. Due to their electrical and optical properties, the materials are used in liquid crystal displays, photovoltaic solar cells, phototransistors, optical heaters, gas sensors, transparent electrodes [3]. At present, CdO and SnO_2 nanoparticles have received considerable attention mainly due to their important potential applications.

Cadmium oxide possesses high transparency in the visible region of solar spectrum and low electrical resistance. Cadmium oxide has metal-like charge transport behaviour with an exceptionally large carrier mobility which is necessary for high transparent conducting oxide materials, especially when low free carrier absorbance is desired [4]. Cadmium oxide is a n-type semiconductor with a direct band gap of 2.5 eV, an indirect band gap of 1.98 eV [5,6]. Cadmium oxide nanoparticles have wide applications based on its specific optical and electrical properties such as diodes, phototransistors, transparent electrodes and sensors [7].

Tin oxide is a n-type semiconductor with high transparency, good electrical conductivity and it exhibit high chemical stability even at high temperature. It has a wide band gap ~3.6 eV at room temperature [8]. Tin oxide nanoparticles have wide range of technological applications such as highly reflective coatings, UV and IR filters, transparent electrodes in solar cells, flat panel displays, and gas sensors [9].

International Journal of Engineering Applied Sciences and Technology, 2016
Vol. 1, Issue 10, ISSN No. 2455-2143, Pages 9-18
Published Online August - September 2016 in IJEAST (http://www.ijeast.com)

The following methods were used to synthesis the metal oxide nanostructures such as sol-gel [10], spray pyrolysis [11], pulsed laser deposition [12], hydrothermal [13], solvothermal [14], microemulsion [15], spray pyrolysis [16] and microwave assisted method [9]. Among the methods mentioned above, microwave assisted synthesis method used in this present work. Microwave assisted synthesis method is comparatively simple, low cost, uniform particle size distribution and offers several advantages over other methods [17-19]. The microwave assisted method offer to larger reaction volumes, allows faster reaction time and remove the need of high temperature injection. The other existing methods demands post synthesis of annealing, huge requirement of time and large energy consumption. But using microwave assisted method, it is possible to synthesize the crystals with good crystalline property without post synthesis of annealing, in less time with low energy consumption.

In this present work, cadmium oxide and tin oxide nanostructures were synthesized by microwave assisted synthesis method. Microstructural properties like strain, dislocation density, number of crystallites; optical properties like reflectance, refractive index, absorption coefficient, extinction coefficient, optical conductivity and dielectric properties like dielectric constant, dielectric losses of CdO and SnO_2 nanostructures were investigated and compared. It is believed such type of research work is more useful for researchers and industrialist for choosing material of their requirements.

II. EXPERIMENTAL

A. Synthesis

All the chemical reagents used in the experiments were obtained from commercial sources and used utilized without further purification. In order to prepare CdO nanostructure, the precursor cadmium acetate dihydrate ($Cd(COOCH_3)_2.2H_2O$) was added to the double distilled water with 0.1 M concentration. The ammonia solution (NH_4OH) was added drop by drop into the above precursor solution and the resulting mixture was stirred at room temperature until the pH of the solution is 8. The obtained precipitate was placed in a microwave oven (2.45 GHz, 800 W) and irradiated for 15 min, finally the precipitate was filtered and dried at 120 °C. Similar procedure was used to synthesize SnO_2 nanostructure and stannous chloride ($SnCl_2.2H_2O$) was taken as precursor material.

B. Characterization

The crystalline structure, average crystalline size of the samples were analyzed by X-ray diffraction (XRD) using a Bruker AXSD8 advance instrument and using the $CuK\alpha_1$ wavelength of 1.5406 Å. TEM analysis was performed on a Philips instrument Model CM12 operating at 120 kV and directly interfaced with a computer for real-time image processing. EDS analysis was observed by JEOL5600LV microscope at an accelerating voltage of 10 kV. The DRS spectra of samples were recorded on a Perkin Elmer UV–visible DRS spectrophotometer. Photoluminescence spectrum was carried out using Spectro flurometer -Fluorolog-FL3-11.

III. RESULTS AND DISCUSSION

A. Structural analysis

Fig. 1(a,b) depicts the XRD patterns of CdO and SnO_2 samples were synthesized by the microwave assisted method. The XRD pattern of CdO nanostructures are shown in Fig. 1a. The diffraction peaks observed at 2θ values of 33.01º, 38.30º, 55.28º, 65.91º and 69.24º correspond to the diffraction lines produced by (111), (200), (220), (311) and (222) planes of the face centered cubic (FCC) structured CdO (JCPDS card No. #65-2908). Further, no traces of impurity phases other than CdO were detected in the XRD pattern, indicating the formation of CdO crystalline phase. The lattice parameter of CdO was found to be a = 4.6699Å and the values are in good agreement with the standard values (JCPDS Card # 78-0653) of cadmium oxide crystals.

Fig. 1b shows the XRD pattern of SnO_2 nanostructures. The diffraction peaks observed at 2θ values of 26.58º, 33.77º, 37.95º, 51.8º, 54.81º, 62º, 64.62º, 66.05º, 71.37º and 78.72º correspond to the diffraction lines produced by [110], [101], [200], [211], [220], [310], [112], [301], [202] and [321] planes of the cassiterite-type tetragonal crystal structured SnO_2 (JCPDS card No. # 41–1445). Further, no traces of impurity phases other than SnO_2 were detected in the XRD pattern, indicating the formation of SnO_2 crystalline phase. The lattice parameters of the microwave irradiated tin oxide samples were calculated as a = 4.7380 Å and c = 3.3502 Å, which matches well with the standard values of tin oxide crystals [20].

International Journal of Engineering Applied Sciences and Technology, 2016
Vol. 1, Issue 10, ISSN No. 2455-2143, Pages 9-18
Published Online August - September 2016 in IJEAST (http://www.ijeast.com)

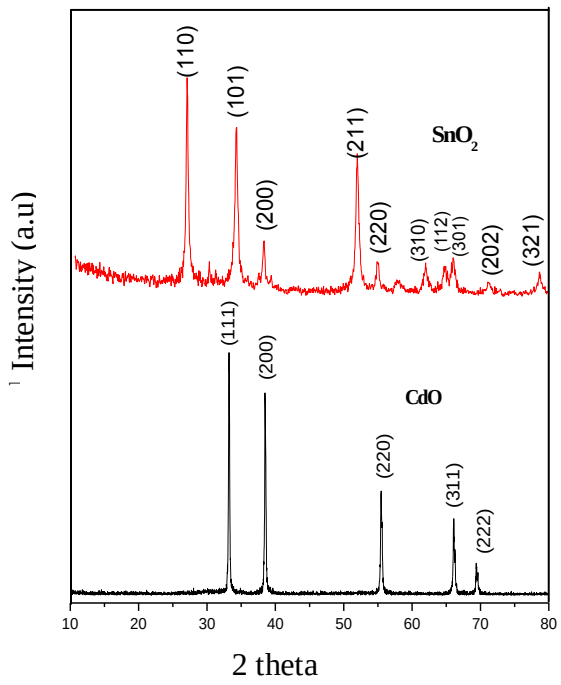

Fig.1. XRD pattern of the CdO and SnO_2 nanostructures

The average crystalline size was determined using the Scherrer's equation

$$D = \frac{0.94\lambda}{\beta \cos\theta} \quad \text{---------- (1)}$$

where λ is the wavelength of incident X-ray, β is the full width at half maximum (FWHM) measured in radians and θ is the Bragg's angle of diffraction peak. The microstructural parameters such as strain (ε), dislocation density (δ) and number of crystallites (N) were determined by using the following formulae:

$$strain(\varepsilon) = \frac{\beta \cos\theta}{4} \quad \text{----------} \quad (2)$$

$$Dislocation\ density(\delta) = \frac{1}{D^2} \text{ ---------- (3)}$$

$$Number\ of\ crystallites(N) = \frac{1}{D^3} \text{ ----------(4)}$$

The crystalline size and the microstructural parameters such as strain, dislocation density and number of crystallites of the CdO and SnO_2 nanostructures were calculated using equations (1 – 4) and the obtained values are presented in Table. 1.

B. Surface morphological analysis

TEM analysis was performed to analyze surface morphology of the CdO and SnO_2 nanostructures and it is shown in Fig. 2a&c. The surface morphology of CdO sample is shown in Fig. 2a. The rod like shaped nanostructures was observed and sizes in the ranges from 5 to 30 nm, thickness 25-40 nm and length is few μm. The TEM micrograph of the SnO_2 sample is shown in Fig. 2c. The presence of less agglomerated spherical

shaped morphology of tin oxide nanostructures was observed. The particle size observed from TEM micrograph is 23 nm.

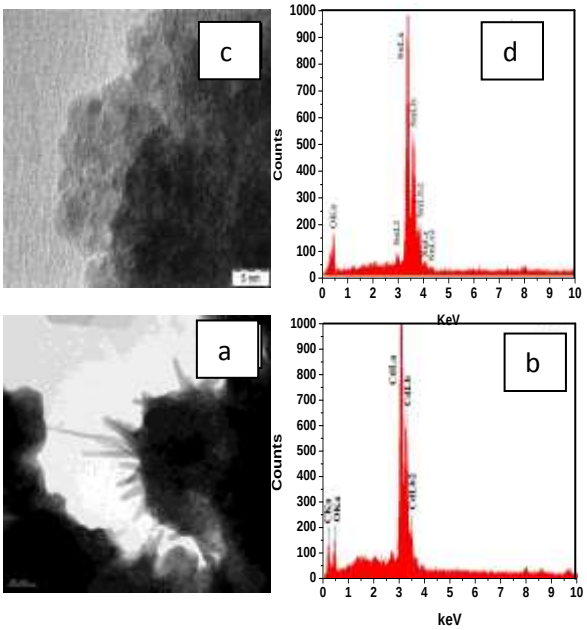

Fig. 2. TEM (a,c) and EDX (b,d) images of the CdO and SnO_2 nanostructures

International Journal of Engineering Applied Sciences and Technology, 2016
Vol. 1, Issue 10, ISSN No. 2455-2143, Pages 9-18
Published Online August - September 2016 in IJEAST (http://www.ijeast.com)

Table.1 Microstructural parameters

Sample	Average crystalline size (nm)	Lattice parameter (Å)	Strain (ε)X10^{-3}	Dislocation density (δ) X10^{15}	Number of crystallites (N)X10^{21}
CdO	51	a = 4.6699	34.70	0.38	7.53
SnO_2	24	a = 4.7380 c = 3.3502	80.28	1.73	72.33

EDS analysis (Fig. 2b&d) was carried out to investigate the elemental composition of CdO and SnO_2 samples. Fig. 2b reports the spectrum of CdO, shows the characteristic peaks associated with O and Cd elements, which confirms the formation of CdO. Small amount of elementary carbon is identified from the figure which is due to produced in result of pyrolysis of format groups [21]. Fig. 2d reports the spectrum of SnO_2, shows the characteristic peaks associated with O and Sn elements, which confirms the formation of SnO_2.

C. Optical studies

The optical constants (reflectance, refractive index, absorbance coefficient, extinction coefficient, real and imaginary parts of optical conductivity) of the microwave irradiated CdO and SnO_2 nanostructures were analyzed and compared using UV-DRS spectra.

Fig. 3 shows the variations of reflectance with wavelength of the CdO and SnO_2 nanostructures. Both samples exhibit similar behavior that is reflectance increases with increase of wavelength. Minimum and maximum reflectance was observed in UV and IR region, respectively. Increase of reflectance with wavelength was observed in visible region. Reflectance of the SnO_2 sample starts to increase at 300 nm but the reflectance of CdO starts to increase at 450 nm. Maximum reflectance (50 %) was observed for CdO sample nearly 800 nm than SnO_2 sample (47 %). Such low reflectance property of the sample makes antireflection coatings and solar thermal applications in flat-plate collectors.

To obtain the optical band gap of CdO and SnO_2 samples, the reflectance values are first converted to absorbance by application of Kubelka–Munk transformation,

$$F(R) = \frac{(1-R)^2}{2R} \qquad \text{---------- (5)}$$

where F(R) is the Kubelka-Munk function and R is the reflectance. The optical band gap is determined from the relation, $(\alpha h\nu) = (h\nu - E_g)^n$, where α is the linear absorption coefficient of the material, Eg is the optical band gap and n is a constant which determines the type of optical transitions.

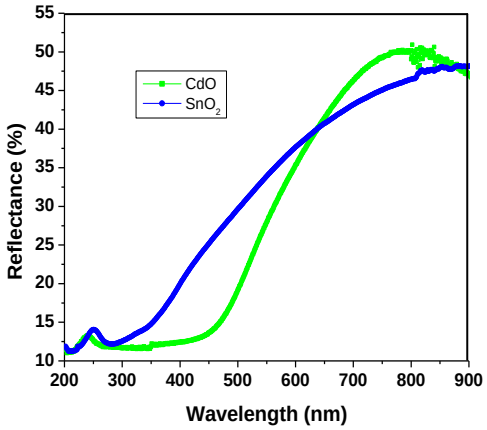

Fig. 3. Variation of the reflectance with wavelengths of CdO and SnO_2 samples

F(R) is directly proportional to the absorbance therefore; F(R) values are converted to the linear absorption coefficient by means of the α= absorbance/t = F(R)/t relation, where t is the thickness of the sample (before analysis the samples were prepared in the form of pellet and measured thickness). The curve of $[F(R)h\nu/t]^2$ vs. hν for the CdO and SnO_2 samples are plotted [22] as shown in Fig. 4. The band gap values were determined by extrapolating the linear portions of these graphs to the energy axis at F(R) = 0 and is found to be 4.20 eV

International Journal of Engineering Applied Sciences and Technology, 2016
Vol. 1, Issue 10, ISSN No. 2455-2143, Pages 9-18
Published Online August - September 2016 in IJEAST (http://www.ijeast.com)

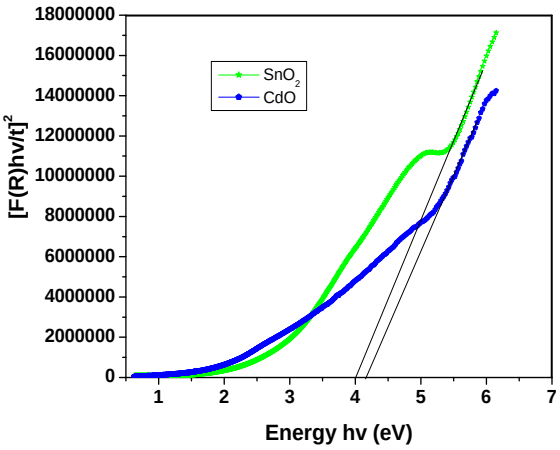

Fig. 4. Variation of $[F(R)hv]^2$ with photon energy (hv) of CdO and SnO_2 samples

and 4 eV for CdO and SnO_2 samples, respectively. The obtained band gap values are higher than the bulk CdO [23-25] and SnO_2 [26-28] samples. The microwave treatment causes the band gap value of both samples get increases. The higher band gap value with effect of microwave irradiation in the present work is believed to be partly due to the Moss-Burstein (M-B) effect. The higher value of optical band gap arises due to improvement in the crystallinity of CdO and SnO_2 samples during microwave irradiation and this confirms the quantum confinement. The present work yields the higher band gap value of microwave irradiated CdO and SnO_2 nanostructure than bulk CdO and SnO_2 without post synthesis of annealing and low energy consumption suggests the material applicable in optoelectronic field. Such kind of higher band gap materials are required for number of optoelectronic applications particularly for solar cell applications.

The refractive index is an important parameter for optical applications. Thus, it is important to determine optical constants of the CdO and SnO_2 samples. The refractive index (n) and extinction coefficient (k) of the CdO and SnO_2 samples are determined by following relation [29,30]:

$$n = \left(\frac{1+R}{1-R}\right) + \left[\frac{4R}{(1-R)^2} - k^2\right]^{1/2} \quad \text{---------- (6)}$$

$$k = \frac{\alpha\lambda}{4\pi} \quad \text{---------- (7)}$$

Fig. 5 shows the variations of refractive index with wavelength of CdO and SnO_2 nanostructures. The refractive index of CdO lies between 2 and 5.99, SnO_2 lies between 2 and 5.05 with respect to the wavelength ranges from 200 – 1000 nm. From both samples, minimum and maximum value of refractive index was observed in UV and IR region, respectively also refractive index rises with wavelength through visible region. The gradual increase of refractive index with wavelength shows normal dispersion. High value of refractive index 5.99 was observed in IR region for CdO sample than SnO_2. The increase of refractive index may be due to the presence of different type of polarizations. The refractive index and reflection spectrum are quite similar due to very small value of extinction coefficient

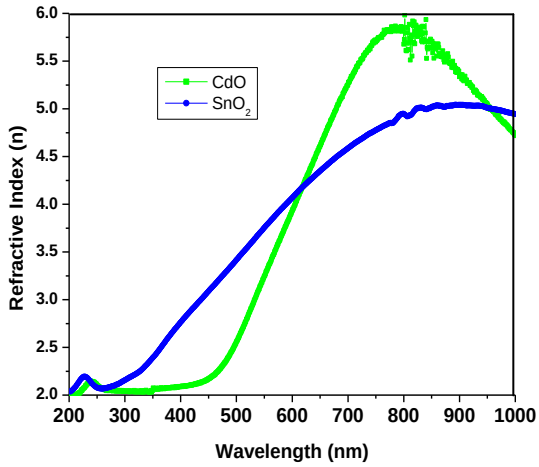

Fig. 5. Variations of refractive index with wavelength of CdO and SnO_2 samples

Fig. 6a shows the variations of absorbance coefficient with wavelength of CdO and SnO_2 samples. The calculated values of absorption coefficient are in the order of 10^2 cm^{-1}. It was observed from Fig. 6a, the absorbance coefficient decreases with wavelength increases. For both samples, small peak was observed in UV region. In the case of SnO_2, after the peak the absorbance coefficient linearly decreases with wavelength increases.

International Journal of Engineering Applied Sciences and Technology, 2016
Vol. 1, Issue 10, ISSN No. 2455-2143, Pages 9-18
Published Online August - September 2016 in IJEAST (http://www.ijeast.com)

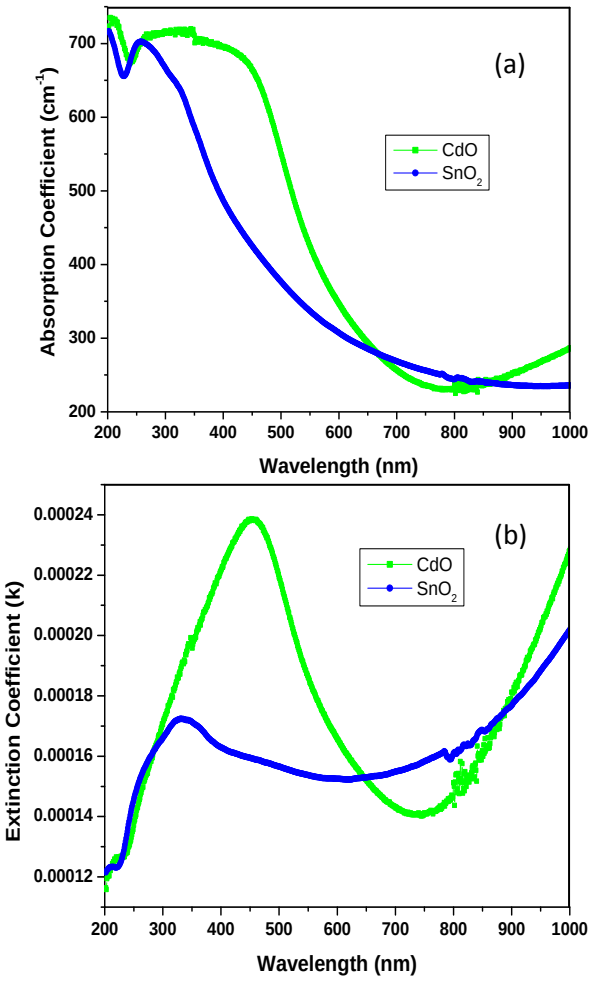

Fig. 6. Variation of absorption coefficient (a) and Extinction coefficient (b) with wavelength of the CdO and SnO_2 samples.

But for CdO, absorbance coefficient is maintained constant up to 450 nm after that decreases gradually. Minimum value of absorbance coefficient was observed nearly 800 nm for CdO and the same minimum value of absorbance coefficient was observed nearly 1000 nm for SnO_2. Fig. 6b shows the variations of extinction coefficient with wavelength of CdO and SnO_2 nanostructures. From Fig. 6b the values of k changed in the range 0.00010 - 0.00025 for CdO and 0.000121 - 0.000221 for SnO_2. Such low value of extinction coefficient represents samples possesses high transmittance. Initially, the value of k increases with increase of wavelength and reaches minimum value again starts to increases with further Increase of wavelength. The extinction coefficient has an inverse relation with the transmittance spectra. Compare to CdO, low value of extinction coefficient is registered for SnO_2. Hence, SnO_2 exhibits high transmittance than CdO.

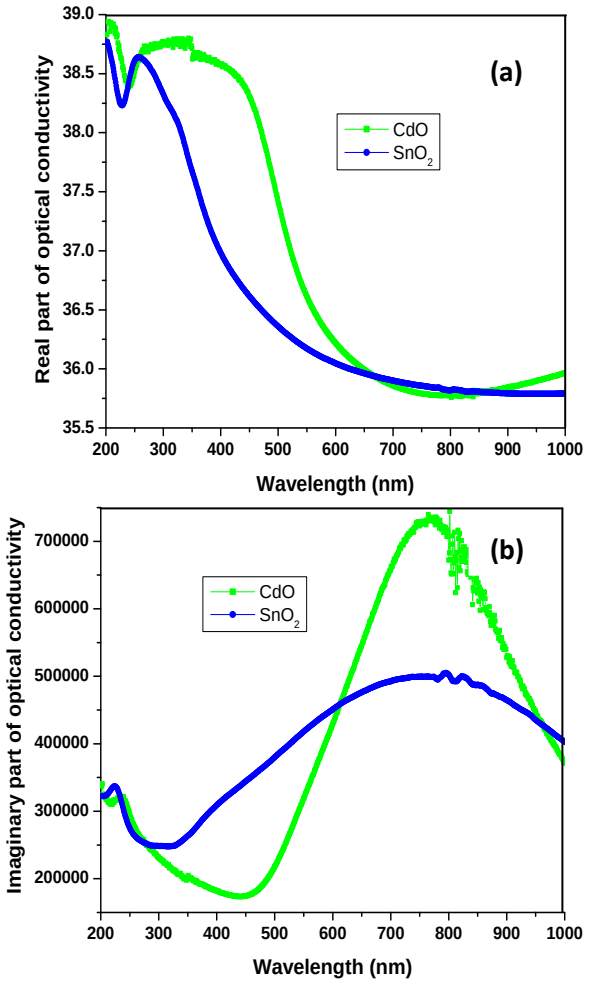

Fig. 7. Variation of real (a) and imaginary (b) part of optical conductivity with wavelength of CdO and SnO_2 samples

The optical conductivity is one of the parameter used to study the optical response of the samples. It is defined as [31,32],

$$\sigma_1 = \omega \varepsilon_2 \varepsilon_0 \quad \text{.....(8)}$$

$$\sigma_2 = \omega \varepsilon_1 \varepsilon_0 \quad \text{.....(9)}$$

International Journal of Engineering Applied Sciences and Technology, 2016
Vol. 1, Issue 10, ISSN No. 2455-2143, Pages 9-18
Published Online August - September 2016 in IJEAST (http://www.ijeast.com)

where, σ_1 is the real part of optical conductivity, σ_2 is the imaginary part of optical conductivity, ω is the angular frequency and ε_0 is the free space dielectric constant.

The variations of real part of the optical conductivity with wavelength of CdO and SnO_2 nanostructures are shown in Fig. 7a. From the figure for both samples, maximum and minimum value of real part of optical conductivity was observed in UV and IR region, respectively. The variations of imaginary part of optical conductivity with wavelength of CdO and SnO_2 nanostructures are shown in Fig. 7b. From the figure for both samples, minimum and maximum value of imaginary part of optical conductivity was observed in UV and IR regions, respectively. After attain the maximum value it starts to decreases towards higher wavelength. Such variation of optical conductivity was believed due to reduction of polarization and crystal defects.

D. Dielectric analysis

The dielectric constant is one of the parameter used to study the electrical response of the samples also it represents the ability of a material to store electrical energy in the presence of an electric field. It is defined as [31],

$$\varepsilon(\omega) = \varepsilon_1(\omega) + i\varepsilon_2(\omega) \quad \text{---------- (10)}$$

where $\varepsilon_1, \varepsilon_2$ are called real and imaginary part of dielectric constants which are related to refractive index (n) and extinction coefficient (k) values. The ε_1 and ε_2 values are calculated using the formulas,

$$\varepsilon_1 = n^2 - k^2 \quad \text{---------- (11)}$$

$$\varepsilon_2 = 2nk \quad \text{---------- (12)}$$

The variation of ε_1 with wavelength of CdO and SnO_2 nanostructures are shown in Fig.8a. From the figure for both samples, low and high value of real part of dielectric constant was observed in UV and IR region, respectively and gradual increase of real part of dielectric constant is observed in visible region. CdO sample exhibits high value of real part of dielectric constant than SnO_2. The variation of ε_2 with wavelength of CdO and SnO_2 nanostructures are shown in Fig. 8b. From the figure for both samples, imaginary part of the dielectric constant linearly increases with wavelength. There is no significance difference of imaginary part of the dielectric constant was observed for both samples.

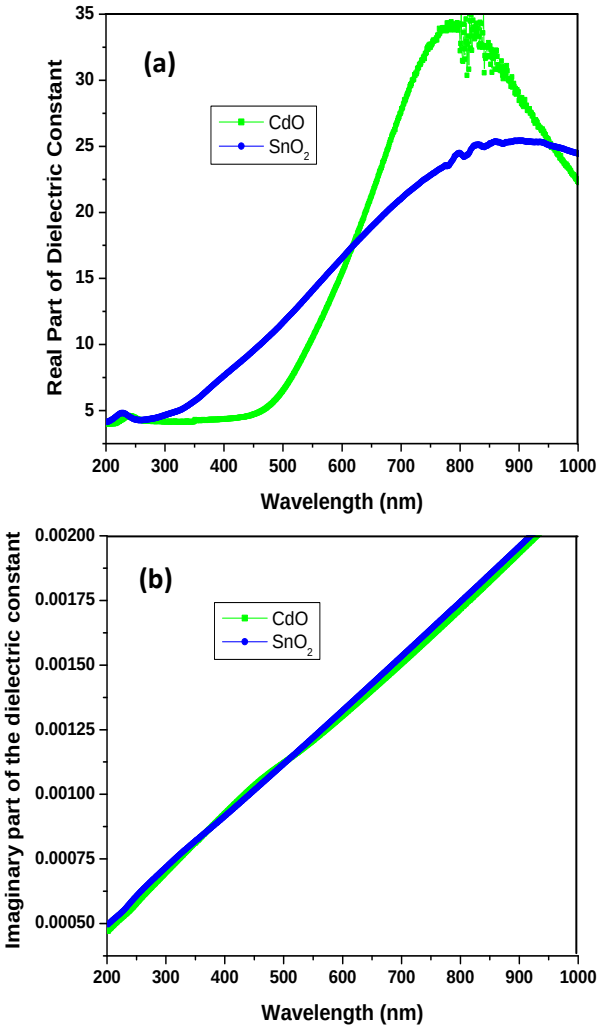

Fig. 8. Variation of real (a) and imaginary (b) part of dielectric constant with wavelength of CdO and SnO_2 samples

From the Fig. 8 (a & b) both real and imaginary part of dielectric constant increases with wavelength increases. However, the value of real part of dielectric constant was higher than that of the imaginary part of dielectric constant. Presence of different type of polarizations and its significance losses at higher frequencies may be the reason for variations of dielectric constant. From the figure, SnO_2 exhibits low dielectric constant than CdO. The optoelectronic materials demands low dielectric constant because such type of material acquired good optical quality with lesser defects. The spectra of real part of dielectric constant is closely similar to spectra

International Journal of Engineering Applied Sciences and Technology, 2016
Vol. 1, Issue 10, ISSN No. 2455-2143, Pages 9-18
Published Online August - September 2016 in IJEAST (http://www.ijeast.com)

of refractive index, this is obtained because of too small value of extinction coefficient.

The dielectric loss is the loss of energy to heating of an object that is made of a dielectric material if a variable voltage is applied to it. Fig. 9 shows the variations of dielectric loss with wavelength of CdO and SnO_2 nanostructures. For both sample, initially dielectric loss increases and attains maximum value with wavelength increases. Further increase of wavelength dielectric loss starts to decreases and reaches the minimum value. It is clearly from the figure, both maximum (0.00022) and minimum (0.000048) value of dielectric constant was observed for CdO in the visible region. The losses due to changes of polarization, the tiny electron shifts can be regarded as an alternating current flow. Such variations of dielectric losses at different wavelengths accounted for some high frequency applications.

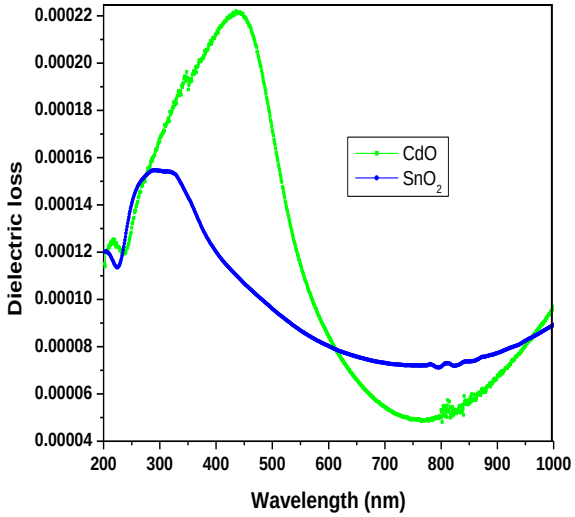

Fig. 9. Variations of dielectric loss with wavelength of CdO and SnO_2 samples

According to equation (3), crystal defect decreases with increase of particle size. Based on that, CdO has less crystal defect than SnO_2. Fig. (3-9) demonstrated the optical properties of CdO and SnO_2 nanostructures. For all the cases, both samples exhibits quite similar behavior follow the same trend. However, based on our experimental conditions, optical properties like reflection, refractive index, absorption coefficient, extinction coefficient, optical conductivity, dielectric constant and dielectric loss of CdO is higher than SnO_2.

E. Photoluminescence analysis

The photoluminescence spectra of the CdO and SnO_2 nanostructures were synthesized by the microwave assisted method at room temperature are shown in Fig. 10. From the photoluminescence spectra of the CdO sample, the emission peak at 471 nm due to artifact which arises because of lamp source [33]. The peak at 528 nm arises due to recombination of a photo generated hole in the valence band with an electron in the conduction band from the oxygen vacancy of the CdO sample [34]. Basically, Vo^0, Vo^+ and Vo^{++} are the possible charge state of oxygen vacancies due to the photo-excitation of SnO_2 the hole might be trapped at the Vo^+ center to

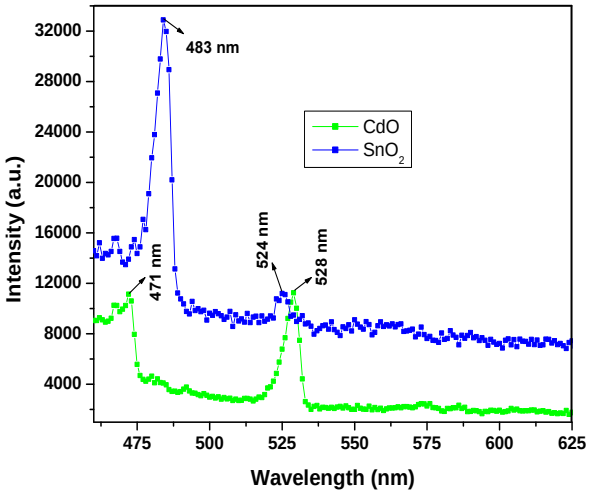

Fig. 10. Photo photoluminescence spectra of the CdO and SnO_2 nanostructures

Vo^{++} center [35,36]. From the photoluminescence spectra of the SnO_2 sample, the emission peak at 483 nm corresponds to blue emission due to single charged oxygen vacancies (Vo) [37].The emission peak at 524 nm is due to the electron transition mediated by defect levels in the band gap such as oxygen vacancies [38].

IV. CONCLUSION

Potentially important metal oxides CdO and SnO_2 were successfully synthesized by microwave assisted technique. XRD pattern reveals that, microwave radiation improves the crystalline property of CdO and SnO_2 nanostructures. Microstructural, optical and dielectric properties of CdO and SnO_2 nanostructures were analyzed and compared. The calculated values

of absorption coefficient for both the samples were in the order of 10^2 cm^{-1}. Refractive index of both samples increases with increase in wavelength confirming the fact that the samples exhibit normal dispersion. The synthesized samples exhibit good optical property which makes them suitable for many applications especially for solar cell applications. Due to their good dielectric properties, low dielectric loss can be used as a promising material for fabrication of dielectric varistors and transparent electrodes in solar cells.

V. REFERENCE

[1] D.M. Carballeda-Galicia, R. Castaneod-Perez, O. Jimenez-Sandoval, S. Jimenez-Sandoval, G. Torres-Delgado, and C.I. Zuniga-Romera, "High transmittance CdO thin films obtained by the sol-gel method," Thin Solid Films, vol. 371, pp. 105-108, August 2000.

[2] Y. Caglar, S. Ilican, and M. Caglar, "Single-oscillator model and determination of optical constants of spray pyrolyzed amorphous SnO_2 thin films," Eur. Phys. J. B, vol. 58, pp. 251-256, September 2007.

[3] R.K. Gupta, K. Ghosh, R. Patel, S.R. Mishra, and P.K. Kahol, "Highly conducting and transparent tin doped CdO thin films for optoelectronic applications," Mater. Lett, vol. 62, pp. 4103 – 4105, September 2008.

[4] T.J. Coutts, D. Young, X. Li, W.P. Mulligan, and X. Wu, "Search for improved transparent conducting oxide . A fundamental investigation of CdO, Cd_2SnO_4, and Zn_2SnO_4," J. Vac. Sci. Technol. A, vol. 18, pp. 2646 – 2660, November 2000.

[5] D.R. Lide (Ed), CRC Handbook of Chemistry and Physics, 77th ed., CRC Press, Boca Raton, 1996/1997, pp. 12/97, 3/278.

[6] K. Gurumurugan, D. Mangalaraj, S. K. Narayandass, K. Sekar, and C.P. Girija Vallabhan, "Characterization of transparent conducting cadmium oxide films deposited by spray pyrolysis," Semicond. Sci. Tech, vol. 9, pp. 1827 – 1832, September 1994.

[7] M. Ristic, S. Popovic, and S. Music, "Formation and properties of $Cd(OH)_2$ and CdO particles," Mater. Lett, vol. 58, pp. 2494 – 2499, August 2004.

[8] S. Goldsmith, E. Cetinorgu, and R.L. Boxman, "Modeling the optical properties of tin oxide thin films," Thin Solid Films, vol. 517, pp. 5146–5150, July 2009.

[9] N. Rajesh, J.C. Kannan, T. Krishnakumar, S.G. Leonardi, and G. Neri, "Sensing behavior to ethanol of tin oxide nanoparticles prepared by microwave synthesis with different irradiation time," Sensor. Actuat. B-chem, vol. 194, pp. 96–104, December 2014.

[10] J.S. Cruz, G.T. Delgado, R.C. Perez, S.J. Sandoval, O.J. Sandoval, C.I.Z. Romero, J.M. Marin, and O.Z. Angel, "Dependence of electrical and optical properties of sol-gel prepared undoped cadmium oxide thin films on annealing temperature," Thin Solid Films, vol. 493, pp. 83 – 87, December 2005.

[11] B.J. Lokhande, P.S. Patil, and M.D. Uplane, "Studies on cadmium oxide sprayed thin films deposited through non-aqueous medium," Mater. Chem. Phys, vol. 84, pp. 238 – 242, April 2004.

[12] M. Yan, M. Lane, C.R. Kannewurf, and R.P.H. Changa, "Highly conductive epitaxial CdO thin films prepared by pulsed laser deposition," Appl. Phys. Lett, vol. 78, pp. 2342, February 2001.

[13] N.S. Baick, G. Sakai, N. Miura, and N. Yamozoe, "Hydrothermally treated sol solution of tin oxide for thin-film gas sensor," Sensor. Actuat. B-chem, vol. 63, pp. 74–79, April 2000.

[14] H. Zhaohui, G. Neng, L. Fanqing, Z. Wanqun, Z. Huaquiao, and Q. Yitai, "Solvothermal preparation and morphological evolution of stannous oxide powders," Mater. Lett, vol. 48, pp. 99–103, March 2001.

[15] K.C. Song, and J.H. Kim, "Synthesis of high surface area tin oxide powders via water-in-oil microemulsions," Powder Technol, vol. 107, pp. 268–272, February 2000.

[16]D. Briand, M. Labeau, J.F. Curie, and G. Delabouglise, "Pd-doped SnO_2 thin films deposited by assisted ultrasonic spraying CVD for gas sensing: selectivity and effect of annealing," Sensor. Actuat. B-chem, vol. 48, pp. 395–402, May 1988.

[17] N. Rajesh, J.C. Kannan, S.G. Leonardi, G. Neri, and T. Krishnakumar, "Investigation of CdO nanostructures synthesized by microwave assisted irradiation technique for NO_2 gas detection," J. Alloy. Compd, vol. 607, pp. 54–60, April 2014.

[18] N. Rajesh, J.C. Kannan, T. Krishnakumar and G. Neri, "Microwave Irradiation Effect on Structural, Optical, and Thermal Properties of Cadmium Oxide Nanostructure," Acta phys. pol. A, vol. 125, pp. 1229 – 1335, May 2014.

[19] N. Rajesh, J.C.Kannan, T.Krishnakumar,

A.Bonavita, S.G.Leonardi, and G.Neri, "Microwave irradiated Sn-substituted CdO nanostructures for enhanced CO_2 sensing," Ceram. Int, vol. 41, pp. 14766–14772, July 2015.

[20] A. Cirera, A. Vila, A. Cornet, and J.R. Morante, "Properties of nanocrystalline SnO obtained by means of microwave process," Mater. Sci. Eng. C, vol. 15, pp. 203 – 205, August 2001.

[21] Barbara Malecka, and Agnieszka Lacz, "Thermal decomposition of cadmium formate in inert and oxidative atmosphere," Thermochimica Acta, vol. 479, pp. 12–16, November 2008.

[22] C.M. Liu, X.T. Zu, Q.M. Wei, and L.M. Wang, "Fabrication and characterization of wire-like SnO_2," J. Phys. D. Appl. Phys, vol. 39, pp. 2494 – 2297, June 2006.

[23] N. Clament Sagaya Selvam, R. Thinesh Kumar, K. Yogeenth, L. John Kennedy, G. Sekaran, and J. Judith Vijaya, "Simple and rapid synthesis of Cadmium Oxide (CdO) nanospheres by a microwave-assisted combustion method," Powder. Technol, vol. 211, pp. 250 – 255, August 2011.

[24] R. Ferro, and J.A. Rodriguez, "Some physical properties of F-doped CdO thin films deposited by spray pyrolysis," Thin Solid Films, vol. 347, pp. 295 – 298, June 1999.

[25] K. Gurumurugan, D. Mangalaraj, SA.K. Narayandass, K. Sekar, and C.P. Girija Vallabhan, "Characterization of Transparent Conducting CdO Films Deposited by Spray Pyrolysis," Semicond. Sci. Tech, vol. 9, pp. 1827 – 1832, September 1994.

[26] T. Krishnakumar, R. Jayaprakash, M. Parthibavarman, A.R. Phani, V.N. Singh, and B.R. Mehta, "Microwave-assisted synthesis and investigation of SnO2 nanoparticles," Mater. Lett, vol. 63, pp. 896 – 898, April 2009.

[27] H. Deng, and J. M. Hossenlopp, "Combined X-ray Diffraction and Diffuse Reflectance Analysis of Nanocrystalline Mixed Sn(II) and Sn(IV) Oxide Powders," J. Phys. Chem. B, vol. 109 pp. 66 – 73, January 2005.

[28] A.S. Ahmed, S. M. Muhamed, M.L. Singla, S. Tabassum, A.H. Naqvi, and A. Azam, "Band gap narrowing and fluorescence properties of nickel doped SnO2 nanoparticles," J. Lumin, vol. 131, pp. 1 – 6, January 2011.

[29] C. Aydın, A. AL. Omar, A. Al-Ghamdi, F. Al-Hazmi, I. S. Yahia, F. El-Tantawy, and F. Yakuphanoglu, "Controlling of crystal size and optical band gap of CdO nanopowder semiconductors by low and high Fe contents," J. Electroceram, vol. 29, pp. 155 – 162, July 2012.

[30] Salih Kose, Ferhunde Atay, Vildan Bilgin, and Idris Akyuz, "In doped CdO films: Electrical, optical, structural and surface properties," Int. J. Hydrogen. Energ, vol. 34, pp. 5260 – 5266, June 2009.

[31] M. Caglar, S. Ilican, Y. Caglar, and Y. Fahrettin, "Electrical conductivity and optical properties of ZnO nanostructured thin film," Appl. Surf. Sci, vol. 255, pp. 4491- 1496, February 2009.

[32]J.N. Hodgson, Optical Absorption and Dispersion in Solids, Chapman and Hall ltd, 11 New fetter Lane London EC4, 1970.

[33] A.S. Lanje, R.S. Ningthoujam, S.J. Sharma, and R.B. Pode, "Luminescence and electrical resistivity properties of cadmium oxide nanoparticles," Indian. J. Pure. & Appl. Physics, vol. 49, pp. 234 – 238, April 2011.

[34] R.S. Ningthoujam, D. Lahiri, V. Sudarsan, H. Poswal, S.K. Kulshreshtha, S.M. Sharma, B. Bhushan, and M.D. Sastry, "Nature of V^{n+} ions in SnO_2: EPR and photoluminescence study," Mater. Res. Bull, vol. 42, pp. 1293 – 1300, July 2007.

[35] F. Yakuphanoglua, S. Ilican, M. Caglar, and Y. Caglar, "Microstructure and electro-optical properties of sol–gel derived Cd-doped ZnO films," Superlattice. Microstr, vol. 47, pp. 732 – 743, June 2010.

[36] M.A. Gondala, Q.A. Drmosha, and T.A. Salehb, "Preparation and characterization of SnO_2 nanoparticles using high power pulsed laser," Appl. Surf. Sci, vol. 256, pp. 7067 – 7070, September 2010.

[37] S. Rani, S.C. Roy, and N. Karar, "Structure, microstructure and photoluminescence properties of Fe doped SnO_2 thin films," Solid State Commun, vol. 141, pp. 214 – 218, January 2007.

[38] M. Gaidi, A. Hajjaji, R. Smirani, B. Bessais, and M.A. El Khakani, "Structure and photoluminescence of ultra thin films of SnO_2 nanoparticles synthesized by means of pulsed laser deposition," J. Appl. Phys, vol. 108, pp. 063537, September 2010.